ple-bond order of the C=N group.

Acknowledgment. This work was supported by CNR (Italy) (Progetto Finalizzato Chimica Fine e Secondaria) and MPI (Italy) grants.

Supplementary Material Available: Tables 1S-6S, giving thermal parameters and complete listings of bond lengths and angles for **2a** and **7a** (8 pages); Tables 7S and 8S, giving observed and calculated structure factors for both complexes (23 pages). Ordering information is given on any current masthead page.

Contribution from the Dipartimento di Chimica Inorganica e Struttura Molecolare, Università di Messina, 98100 Messina, Italy, and Dipartimento di Chimica, Università di Siena, 53100 Siena, Italy

Chemical Oxidation of Binuclear Rhodium(I) Complexes with Silver Salts. Synthesis, X-ray Crystal Structure, and Electrochemical Properties of the Rh_2^{4+} Mixed-Ligand Complex $Rh_2(Form)_2(O_2CCF_3)_2(H_2O)_2 \cdot 0.5C_6H_6$ (Form = *N*,*N*'-Di-*p*-tolylformamidinate Anion)

Pasquale Piraino,*† Giuseppe Bruno,† Giuseppe Tresoldi,† Sandra Lo Schiavo,† and Piero Zanello*‡

Received April 3, 1986

The facile chemical oxidation of the binuclear rhodium(I) formamidinate complex $[Rh(C_8H_{12})(Form)]_2$ (Form = $[p\text{-}CH_3C_6H_4NC(H)NC_6H_4CH_3\text{-}p]^-$) with AgO_2CCF_3 (mole ratio 1:4) yields the mixed-ligand Rh_2^{4+} complex $Rh_2(Form)_2(O_2CCF_3)_2(H_2O)_2$. The complex reacts with Lewis bases such as pyridine, dimethyl sulfoxide, piperidine, and 4-methylimidazole to produce stable 1:2 axial adducts. The crystal structure has been determined by X-ray diffraction analysis. The green crystals are triclinic, space group $P\bar{1}$, with a = 10.467 (1) Å, b = 13.151 (1) Å, c = 15.470 (2) Å, α = 70.68 (2)°, β = 88.89 (4)°, γ = 79.16 (3)°, V = 1971.6 Å^3, Z = 2, D_{calcd} = 1.609 g cm^{-3}, R = 0.032, and R_w = 0.034. The molecule consists of two formamidinate and two trifluoroacetate groups symmetrically disposed about the Rh-Rh unit in the conventional fashion. Two water molecules are axially bonded at 2.315 (3) Å from the rhodium atoms. The striking features of the structure are the lengthening of the Rh-Rh (2.425 (1) Å) and Rh-O_{eq} (2.082 (3) Å) bond distances with respect to the analogous $Rh_2(O_2CCF_3)_4(H_2O)_2 \cdot 2DTBN$ and the cisoid arrangement of the formamidinate groups. The Rh-Rh-O_{ax} angles deviate significantly from linearity (167.9 (1) and 169.3 (1)°) as a consequence of steric interactions between the tolyl fragments and the water molecules that participate in hydrogen-bonding interactions throughout the crystal lattice. The electrochemistry in different nonaqueous solvents points out the ability of the title complex to undergo two subsequent one-electron reversible or quasi-reversible anodic processes, attributable to the $Rh^{II}Rh^{II}/Rh^{II}Rh^{III}$ and $Rh^{II}Rh^{III}/Rh^{III}Rh^{III}$ charge transfers, respectively. As expected, these anodic processes are easier than in the case of the corresponding tetracarboxylato species. Of the two electrogenerable anodic products, only the mixed-valence $Rh^{II}Rh^{III}$ derivative is fully stable, and its stability has been quantitatively evaluated and discussed also with respect to that of the other dirhodium complexes.

Introduction

Binuclear rhodium complexes containing the Rh_2^{4+} core have been the center of many experimental and theoretical studies.[1] For the most part, these have been directed toward complexes containing four carboxylate groups as bridging ligands. Up to now only few Rh_2^{4+} complexes containing mixed[2] or non-carboxylate bridging ligands[3] have been isolated and structurally characterized. The presence of bridging ligands other than carboxylate allows a greater variation in the molecular orbital patterns and hence the chemical reactivity of the Rh_2^{4+} complexes. As elegantly pointed out by the electrochemical studies of Kadish, Bear, and co-workers, a dramatic variation is seen in the redox potential of the couple $Rh^{II}Rh^{II}/Rh^{II}Rh^{III}$ as a consequence of the gradual replacement of oxygen atoms by NH groups.[4] In some cases the $Rh^{II}Rh^{III}/Rh^{III}Rh^{III}$ couples showed anodic behavior. Also the complex $Rh_2(N_2R_2CR)_4$ (R = phenyl) undergoes a quasi-reversible reduction leading to the formation of a formal $Rh^{II}Rh^{I}$ derivative.[3d]

In this paper we report the synthesis, structure analysis, and electrochemistry of the Rh_2^{4+} mixed-ligand complex $Rh_2(Form)_2(O_2CCF_3)_2(H_2O)_2$ (Form = $[p\text{-}CH_3C_6H_4NC(H)NC_6H_4CH_3\text{-}p]^-$) obtained by chemical oxidation with silver trifluoroacetate of the binuclear rhodium(I) complex $[Rh(C_8H_{12})(Form)]_2$. A similar synthetic route has been successfully used to prepare the Rh_2^{5+} complex $Rh_2(Form)_3(NO_3)_2$.[5]

Experimental Section

Starting Materials. $[Rh(C_8H_{12})(Form)]_2$ was prepared by the literature procedure.[6] 4-Methylimidazole (4-MeIm) and silver trifluoroacetate were purchased from Aldrich Chemical Co. and used as received. The supporting electrolytes tetraethylammonium perchlorate, $[NEt_4]ClO_4$ (Carlo Erba), and tetrabutylammonium perchlorate, $[NBu_4]ClO_4$ (Fluka), were dried in a vacuum oven at 100 °C and used without further purification. The solvents used for electrochemistry (dichloromethane, acetonitrile, acetone, tetrahydrofuran, *N*,*N*-dimethylformamide, dimethyl sulfoxide (Burdick and Jackson); nitromethane, benzonitrile (Aldrich)) were of "distilled in glass" grade and used as received.

Apparatus. Infrared spectra were recorded on KBr pellets with a Perkin-Elmer 783 instrument. Electronic absorption spectra were run as benzene solutions on a Perkin-Elmer Lambda 5 UV-visible spectrophotometer. ESR experiments were performed on a Bruker ER 200D-SRC X-band spectrometer. Elemental analyses were performed by the Microanalytical Laboratory of the Organic Chemistry Institute of Milan and Analytische Labortorien Malissa and Reuter, Elbach, West Germany. The electrochemical apparatus has been described elsewhere.[7] Potential values are referred to an aqueous saturated calomel reference

† Università di Messina.
‡ Università di Siena.

(1) (a) Felthouse, T. R. *Prog. Inorg. Chem.* **1982**, *20*, 109. (b) Boyer, E. B.; Robinson, S. D. *Coord. Chem. Rev.* **1983**, *50*, 109. (c) Cotton, F. A.; Walton, R. A. *Multiple Bonds between Metal Atoms*; Wiley-Interscience: New York, 1982; p 311.
(2) (a) Cotton, F. A.; Thompson, S. L. *Inorg. Chim. Acta* **1984**, *81*, 193. (b) Cotton, F. A.; Felthouse, T. R. *Inorg. Chem.* **1981**, *20*, 584. (c) Chakravarty, A. R.; Cotton, F. A.; Tocher, A. D. Tocher, S. H. *Organometallics* **1985**, *4*, 8.
(3) (a) Dennis, A. M.; Korp, J. D.; Bernal, I.; Howard, R. A.; Bear, J. L. *Inorg. Chem.* **1983**, *22*, 1522. (b) Chakravarty, A. R.; Cotton, F. A.; Tocher, A. D.; Tocher, S. H. *Inorg. Chim. Acta* **1985**, *101*, 185. (c) Barrow, A. R.; Wilkinson, G.; Motevalli, M.; Hursthouse, M. B. *Polyhedron* **1985**, *4*, 1131. (d) Le, J. C.; Chavan, M. Y.; Chau, L. K.; Bear, J. L.; Kadish, K. M. *J. Am. Chem. Soc.* **1985**, *107*, 7195.
(4) Chavan, M. Y.; Zhu, T. P.; Lin, X. Q.; Ahsan, M. Q.; Bear, J. L.; Kadish, K. M. *Inorg. Chem.* **1984**, *23*, 4538.
(5) Piraino, P.; Bruno, G.; Faraone, F.; Lo Schiavo, S. *Inorg. Chem.* **1985**, *24*, 4760.
(6) Piraino, P.; Tresoldi, G.; Faraone, F. *J. Organomet. Chem.* **1982**, *224*, 305.
(7) Zanello, P.; Leoni, P. *Can. J. Chem.* **1985**, *63*, 922.

0020-1669/87/1326-0091$01.50/0

electrode (SCE). Extra-pure nitrogen was employed to remove oxygen from tested solutions.

Synthesis of $Rh_2(Form)_2(O_2CCF_3)_2(H_2O)_2$ (1). In a vessel protected from the light, a quantity of silver trifluoroacetate (0.40 g, 1.84 mmol) in 2 mL of water was added to a solution of $[Rh(C_8H_{12})(Form)]_2$ (0.40 g, 0.46 mmol) in 50 mL of a CH_2Cl_2–CH_3OH (1:1) mixture. The color of the solution immediately changed from yellow-orange to green and was accompanied by the formation of a gray precipitate of silver metal. The slurry was allowed to stir for about 4 h, during which time the color changed from green to blue-violet. The resultant solution was filtered on a short Celite column to remove the silver and concentrated to one-third volume under vacuum. A violet compound (0.25 g) was deposited overnight at room temperature. The complex was identified as $Rh_2(Form)_2(O_2CCF_3)_2(CH_3OH)_2$ by elemental analysis and IR spectroscopy. The crystallization of the methanol adduct from a benzene–heptane solution (1:2) gave 0.24 g of the water adduct (57%) as green crystals. Anal. Calcd for $Rh_2C_{34}H_{34}N_4F_6O_6$: C, 44.66; H, 3.74; N, 6.12; F, 12.46. Found: C, 44.85; H, 3.80; N, 6.17; F, 12.30. Infrared spectrum (KBr pellet, cm^{-1}): $\nu_{asym}(H_2O)$ 3610 (w), 3520 (w); $\nu_{asym}(CO_2)$ 1655 (s); $\nu(N{-}C{-}N)$ 1570 (s). Electronic spectrum (benzene solution; λ_{max}, nm (ϵ, M^{-1} cm^{-1})): 652 (457), 439 (863), 539 (sh) (496).

Synthesis of $Rh_2(Form)_2(O_2CCF_3)_2(py)_2$ (2). To a benzene solution of $Rh_2(Form)_2(O_2CCF_3)_2(H_2O)_2$ (0.10 g, 0.10 mmol) was added 0.1 mL of pyridine (py), changing the color of the solution immediately to pink-red. After 10 min the volatiles were removed, leaving a red solid that was crystallized from benzene–heptane (1:1), giving 0.090 g of the pyridine adduct. Anal. Calcd for $Rh_2C_{44}H_{40}N_6F_6O_4$: C, 50.98; H, 3.88; N, 8.10; F, 10.99. Found: C, 51.10; H, 3.92; N, 7.98; F, 11.10. Infrared spectrum (KBr pellet, cm^{-1}): $\nu_{asym}(CO_2)$ 1660 (s); $\nu(N{-}C{-}N)$ 1580 (s).

Synthesis of $Rh_2(Form)_2(O_2CCF_3)_2(Me_2SO)_2$ (3). A procedure similar to that for the pyridine adduct was followed with use of dimethyl sulfoxide. Workup as above led to the formation of 0.075 g of red-orange crystals. Anal. Calcd for $Rh_2C_{38}H_{42}N_4F_6S_2O_6$: C, 44.11; H, 4.09; N, 5.41; S, 6.19. Found: C, 44.35; H, 4.15; N, 5.40; S, 6.32. Infrared spectrum (KBr pellet, cm^{-1}): $\nu_{asym}(CO_2)$ 1660 (s); $\nu(N{-}C{-}N)$ 1575 (s); $\nu(SO)$ 1015 (s).

Synthesis of $Rh_2(Form)_2(O_2CCF_3)_2(pip)_2{\cdot}0.5C_6H_{14}$ (4). The complex $Rh_2(Form)_2(O_2CCF_3)_2(H_2O)_2$ (0.10 g, 0.1 mmol) was dissolved in 10 mL of diethyl ether and stirred with 2 mmol equiv of piperidine (pip) for 15 min to give a red-orange solution. Addition of 10 mL of hexane followed by slow evaporation of the solvent gave 0.095 g of the complex **4**. Anal. Calcd for $Rh_2C_{47}H_{59}N_6F_6O_4$: C, 51.70; H, 5.44; N, 7.69; F, 10.43. Found: C, 51.90; H, 5.37; N, 7.62; F, 10.52. Infrared spectrum (KBr pellet, cm^{-1}): $\nu_{asym}(CO_2)$ 1650 (s); $\nu(N{-}C{-}N)$ 1570 (s).

Synthesis of $Rh_2(Form)_2(O_2CCF_3)_2(4\text{-}MeIm)_2$ (5). This complex was obtained in exactly the same way as the analogous complex **4** by starting from $Rh_2(Form)_2(O_2CCF_3)_2(H_2O)_2$ (0.10 g, 0.10 mmol) and 4-methylimidazole (mole ratio 1:2); yield 95%. Anal. Calcd for $Rh_2C_{42}H_{42}N_8F_6O_4$: C, 48.88; H, 4.06; N, 10.74; F, 10.92. Found: C, 48.50; H, 3.99; N, 10.64; F, 11.06. Infrared spectrum (KBr pellet, cm^{-1}): $\nu_{asym}(CO_2)$ 1655 (s); $\nu(N{-}C{-}N)$ 1580 (s).

X-ray Data Collection and Structure Refinement. Data were collected on a Siemens-Stoe four-circle diffractometer at room temperature using Mo Kα radiation (λ = 0.71069 Å). Accurate unit cell dimensions and crystal orientation matrices were obtained from least-squares refinement of 2θ, ω, χ, and ϕ values of 20 reflections in the range $18 < 2\theta < 34°$.

The compound crystallizes in the triclinic space group $P\bar{1}$, with a = 10.467 (1) Å, b = 13.151 (1) Å, c = 15.470 (2) Å, α = 70.68 (2)°, β = 88.89 (4)°, γ = 79.16 (3)°, V = 1971.6 Å^3, Z = 2, and D_{calcd} = 1.609 g cm^{-3}. Lorentz and polarization corrections were applied, but not absorption (μ = 8.98 cm^{-1}). The structure was solved with use of standard Patterson methods and refined on F by blocked-matrix least-squares (three blocks); metal atoms were included in all cycles. All non-hydrogen atoms were refined anisotropically, while hydrogen atoms were included in the scattering model in calculated idealized positions (C–H = 0.98 Å) with a common thermal parameter. Hydrogen atoms of water molecules were located in the difference Fourier and refined isotropically. Of 8611 independent reflections, measured with an ω/θ scan technique in the range $3 < 2\theta < 54$, 5162 have $I > 3\sigma(I)$ were used to refine 529 parameters to final residuals of $R = (\sum||F_o| - |F_c||)/\sum|F_o| = 0.032$ and $R_w = (\sum w(|F_o| - |F_c|)^2/\sum w|F_o|^2)^{1/2} = 0.034$ ($w = 1.586/(\sigma^2(F_o) + 0.000292F_o^2)$). Atomic scattering factors were taken from ref 8 and anomalous scattering of rhodium from ref 9. All the calculations were performed with the SHELX 76 set of programs[10] on the IBM 4341 computer of the "Centro di calcolo dell'Università" di Messina.

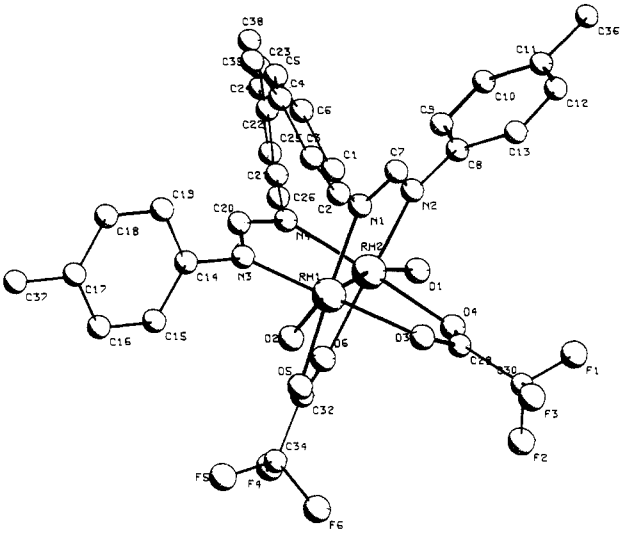

Figure 1. Molecular structure of $Rh_2(Form)_2(O_2CCF_3)_2(H_2O)_2$ with atomic labels.

Distances and angles associated with the tolyl and trifluoroacetate fragments (Table V), hydrogen atom parameters (Table VI), temperature factors (Table VII), and structure factors have been deposited as supplementary material.

Results and Discussion

The infrared spectrum of the title complex shows, in the region 1700–1500 cm^{-1}, the expected $\nu_{asym}(CO_2)$ and $\nu(N{-}C{-}N)$ stretching frequencies at 1655 and 1570 cm^{-1}, respectively; two weak bands at 3610 and 3520 cm^{-1} indicate the asymmetric and symmetric stretchings of the coordinated water. The ^1H NMR spectrum in $CDCl_3$ reveals for the methyl protons only one signal at δ 2.15, pointing out the symmetric arrangement of the formamidinate ligands about the Rh–Rh unit. The electronic spectrum, recorded in benzene, exhibits, in the visible region, two absorptions with maxima at 652 nm (ϵ = 457 M^{-1} cm^{-1}) and 439 nm (ϵ = 863 M^{-1} cm^{-1}) with a shoulder at 539 nm (ϵ = 496 M^{-1} cm^{-1}). The assignment of these electronic transitions is uncertain and cannot be inferred in the absence of theoretical studies.

The title complex is readily soluble in a variety of solvents including acetonitrile (MeCN), dimethyl sulfoxide (Me_2SO), pyridine (py), dimethylformamide (DMF), and tetrahydrofuran (THF), giving deeply colored solutions. From these solutions only the 1:2 adducts with pyridine and Me_2SO were isolated and characterized. The other adducts were not isolated because the solids obtained revert rapidly to the green water adduct. The IR spectra (Nujol mull) show the stretches characteristic of the bridging trifluoroacetate and formamidinate groups at frequencies comparable with those of the aquo complex, indicating that axial adducts (class I) are formed. The red-orange dimethyl sulfoxide derivative shows in the IR spectrum a band assignable to $\nu(SO)$ stretching at 1015 cm^{-1}, only slightly shifted to lower frequencies in respect to the uncoordinated Me_2SO. On these bases we cannot assign the coordination mode of Me_2SO although the color of the adduct could suggest a S-bound Me_2SO. It is worthwhile mentioning that the complex $Rh_2(O_2CCF_3)_4$ forms with Me_2SO an oxygen-bound adduct and with pyridine a 4:1 adduct with the pyridines bound both axially and equatorially (class III).[11] To confirm this divergence in reactivity with the tetrakis(trifluoroacetate) derivative, the title complex forms stable 1:2 axial adducts (class I) with piperidine and 4-methylimidazole.

The oxidation of the rhodium(I) complex $[Rh(C_8H_{12})(Form)]_2$ takes place with an obscure course as pointed out by the ratio Rh:oxidant. In fact, when the reaction is carried out with the ratio Rh:Ag = 1:1, an initial green color immediately develops and silver metal is formed. Shortly after, the solution becomes yellow-brown and a mixture of products, which we were unable to isolate in a

(8) Cromer, D. T.; Libemann, D. *J. Chem. Phys.* **1970**, *53*, 1981.
(9) Stewart, R. F. *J. Chem. Phys.* **1970**, *53*, 3175.
(10) Sheldrick, G. M. "SHELX 76 Computing System of Crystallography Programs"; University of Cambridge: Cambridge, England, 1976.
(11) Telser, J.; Drago, R. S. *Inorg. Chem.* **1984**, *23*, 2599.

Table I. Selected Bond Lengths (Å), Interbond Angles (deg), and Relevant Torsion Angles (deg)

Distances			
Rh (1)–Rh (2)	2.425 (1)		
Rh(1)–O(2)	2.311 (3)	Rh(2)–O(1)	2.319 (3)
–O(3)	2.087 (3)	–O(4)	2.079 (3)
–O(5)	2.073 (3)	–O(6)	2.092 (4)
–N(1)	1.996 (4)	–N(2)	1.998 (4)
–N(3)	1.987 (3)	–N(4)	1.990 (3)
O(3)–C(28)	1.242 (6)	O(4)–C(28)	1.239 (5)
O(5)–C(32)	1.241 (6)	O(6)–C(32)	1.239 (5)
N(1)–C(7)	1.315 (6)	N(2)–C(7)	1.305 (6)
N(3)–C(20)	1.303 (5)	N(4)–C(20)	1.309 (6)
N(1)–C(1)	1.420 (6)	N(2)–C(8)	1.415 (6)
N(3)–C(14)	1.411 (6)	N(4)–C(21)	1.417 (5)
Angles			
O(2)–Rh(1)–Rh(2)	169.3 (1)	Rh(1)–Rh(2)–O(1)	167.9 (1)
N(1)–Rh(1)–N(3)	90.0 (2)	–N(4)	87.6 (1)
O(5)–Rh(1)–N(1)	175.4 (1)	–N(2)	88.6 (1)
–N(3)	89.8 (2)	–O(6)	86.8 (1)
O(3)–Rh(1)–N(3)	175.4 (1)	–O(4)	87.2 (1)
–N(1)	91.8 (1)	N(2)–Rh(2)–N(4)	90.1 (2)
–O(5)	88.1 (1)	O(6)–Rh(2)–N(4)	90.8 (2)
O(2)–Rh(1)–N(3)	94.3 (1)	O(6)–Rh(2)–N(2)	175.2 (1)
–N(1)	102.5 (1)	O(4)–Rh(2)–N(4)	174.7 (1)
–O(5)	82.1 (1)	–N(2)	90.3 (1)
–O(3)	89.5 (1)	–O(6)	88.3 (1)
Rh(2)–Rh(1)–N(3)	88.5 (1)	O(1)–Rh(2)–N(4)	102.5 (1)
–N(1)	87.8 (1)	–N(2)	98.0 (1)
–O(5)	87.6 (1)	–O(6)	86.4 (1)
–O(3)	87.3 (1)	–O(4)	82.7 (1)
Rh(1)–O(3)–C(28)	117.1 (3)	Rh(2)–O(4)–C(28)	117.9 (3)
Rh(1)–O(5)–C(32)	117.5 (3)	Rh(2)–O(6)–C(32)	117.5 (3)
Rh(1)–N(1)–C(7)	119.0 (3)	Rh(2)–N(2)–C(8)	126.0 (3)
–C(1)	123.5 (3)	–C(7)	118.1 (3)
C(1)–N(1)–C(7)	115.9 (4)	C(7)–N(2)–C(8)	115.8 (4)
Rh(1)–N(3)–C(20)	118.3 (3)	Rh(2)–N(4)–C(21)	123.5 (3)
–C(14)	122.7 (3)	–C(20)	119.4 (3)
N(1)–C(7)–N(2)	124.8 (4)	N(3)–C(20)–N(4)	124.5 (4)

Torsion Angles	
N(3)–Rh(1)–Rh(2)–N(4)	9.4 (2)
N(1)–Rh(1)–Rh(2)–N(2)	9.5 (2)
O(5)–Rh(1)–Rh(2)–O(6)	8.3 (1)
O(3)–Rh(1)–Rh(2)–O(4)	8.0 (1)
Rh(1)–N(3)–C(14)–C(19)	105.1 (5)
Rh(1)–N(1)–C(1)–C(2)	62.8 (6)
Rh(2)–N(2)–C(8)–C(9)	54.0 (6)
Rh(2)–N(4)–C(21)–C(26)	63.9 (5)

Table II. Nonbonded Intermolecular Distances (Å)[a] Less Than 3.6 Å

O(1)···O(1)^{i}	3.354 (5)[b]	F(1)–C(16)^{iii}	3.554 (9)
O(1)···O(6)^{i}	3.055 (5)[b]	F(3)–C(17)^{ii}	3.333 (6)
O(2)···O(2)^{ii}	3.077 (4)[b]	F(3)–C(18)^{ii}	3.330 (6)
O(2)···O(3)^{ii}	2.870 (5)[b]	F(4)–C(9)^{i}	3.263 (8)
O(1)–F(4)^{i}	3.173 (5)[b]	F(4)–C(10)^{i}	3.123 (8)
O(1)–C(26)^{i}	3.470 (7)	F(6)–C(5)^{iv}	3.423 (7)
O(2)–F(3)^{ii}	3.253 (5)	F(6)–C(25)^{i}	3.545 (8)
F(1)–F(5)^{iii}	3.201 (6)		

[a] Symmetry transformations: (i) $-x + 1, -y, -z$; (ii) $-x + 1, -y, -z + 1$; (iii) $x + 1, y, z$; (iv) $x, y - 1, z$. [b] Hydrogen bonds.

pure form, was recovered. Furthermore, when the reaction is performed with the ratio 1:3, the title complex is still obtained and no further oxidation takes place.

Crystal Structure of $Rh_2(Form)_2(O_2CCF_3)_2(H_2O)_2$. The molecule is illustrated in Figure 1 together with the atomic numbering scheme. Selected bond distances (Å) and angles (deg) as well as relevant torsion angles are reported in Table I. Contacts less than 3.6 Å and hydrogen bonding are listed in Table II. Final positional parameters are reported in Table III.

The molecule consists of a Rh_2^{4+} core symmetrically surrounded by pairs of trifluoroacetate and formamidinate groups in a cisoid arrangement. The roughly octahedral coordination of each rhodium atom is completed by the axial coordination of two water molecules. The structure is completed by a benzene molecule of crystallization located on an inversion center. The molecular packing is mainly determined by van der Waals and hydrogen interactions.

Table III. Fractional Coordinates ($\times 10^4$) for Non-Hydrogen Atoms

atom	*x/a*	*y/b*	*z/c*
Rh(1)	4412 (1)	722 (1)	2071 (1)
Rh(2)	5210 (1)	846 (1)	1564 (1)
O(1)	6162 (3)	578 (3)	272 (2)
O(2)	3637 (3)	270 (3)	4532 (2)
O(3)	6220 (3)	−248 (2)	3611 (2)
O(4)	6830 (3)	−315 (2)	2230 (2)
O(5)	3796 (3)	−697 (2)	3099 (2)
O(6)	4268 (3)	−446 (2)	1633 (2)
F(1)	9217 (3)	−1108 (4)	3121 (3)
F(2)	8126 (4)	−2346 (3)	3429 (3)
F(3)	8361 (4)	−1564 (3)	4372 (2)
F(4)	3152 (6)	−2063 (4)	1691 (3)
F(5)	2222 (5)	−1958 (4)	2856 (3)
F(6)	4078 (6)	−2810 (3)	2954 (4)
N(1)	5055 (4)	2098 (3)	2943 (2)
N(2)	6088 (4)	2053 (3)	1610 (2)
N(3)	2715 (4)	1609 (3)	2468 (2)
N(4)	3590 (4)	1938 (3)	1040 (2)
C(28)	6955 (5)	−567 (3)	3074 (3)
C(30)	8177 (5)	−1403 (4)	3509 (3)
C(32)	3825 (5)	−914 (4)	2376 (3)
C(34)	3273 (7)	−1913 (5)	2443 (4)
C(35)	2997 (10)	5059 (6)	4826 (5)
C(36)	9632 (7)	4147 (7)	−883 (5)
C(37)	−1778 (6)	2160 (6)	4530 (5)
C(38)	2957 (8)	4738 (6)	−2687 (4)
C(1)	4544 (5)	2831 (4)	3418 (3)
C(2)	4641 (5)	2495 (4)	4358 (3)
C(3)	4132 (6)	3230 (5)	4795 (3)
C(4)	3530 (7)	4288 (5)	4317 (4)
C(5)	3459 (6)	4605 (4)	3393 (4)
C(6)	3956 (5)	3886 (4)	2933 (3)
C(7)	5787 (4)	2480 (3)	2255 (3)
C(8)	7002 (4)	2516 (3)	991 (3)
C(9)	6702 (5)	2920 (4)	68 (3)
C(10)	7569 (5)	3432 (4)	−529 (3)
C(11)	8720 (5)	3561 (5)	−227 (4)
C(12)	8988 (5)	3176 (5)	698 (4)
C(13)	8163 (5)	2635 (4)	1305 (3)
C(14)	1588 (4)	1757 (4)	2962 (3)
C(15)	938 (5)	923 (4)	3334 (4)
C(16)	−151 (6)	1060 (5)	3838 (4)
C(17)	−610 (5)	2029 (5)	3975 (3)
C(18)	48 (6)	2858 (5)	3603 (4)
C(19)	1147 (5)	2730 (4)	3109 (4)
C(20)	2660 (5)	2105 (3)	1584 (3)
C(21)	3429 (4)	2643 (3)	116 (3)
C(22)	3272 (5)	3754 (4)	−105 (3)
C(23)	3128 (5)	4419 (4)	−1000 (4)
C(24)	3134 (5)	3996 (5)	−1697 (3)
C(25)	3307 (5)	2890 (5)	−1472 (3)
C(26)	3449 (5)	2199 (4)	−573 (3)
C(40)	10644 (8)	647 (6)	−703 (6)
C(41)	9921 (9)	143 (8)	838 (6)
C(42)	10591 (9)	796 (7)	140 (7)

The most striking structural features are the length of Rh–Rh bond and the cisoid arrangement of the bridging ligands. The value of 2.425 (1) Å found for the Rh–Rh distance is well in the range observed for other Rh_2^{4+} carboxylate complexes.[1] But for comparative purposes it is more informative to consider the complex $Rh_2(O_2CCF_3)_4(H_2O)_2 \cdot 2DTBN$[12] (DTBN = di-*tert*-butyl nitroxide). The substitution of a pair of trifluoroacetate groups in the previously cited complex with two formamidinate groups leads to the lengthening of the Rh–Rh and Rh–O_{eq} bond distances. The elongation of the Rh–Rh bond of 0.02 Å can be ascribed to the constraining effect of the formamidinate ligands while the lengthening of the Rh–O_{eq} distances, which range from 2.073 to

(12) Cotton, F. A.; Felthouse, T. R. *Inorg. Chem.* **1982**, *21*, 2667.

2.092 Å (mean value 2.036 (2) Å in the tetrakis(trifluoroacetate) complex), is a direct consequence of the trans influence of the nitrogen atoms of the formamidinate ligands. The two rhodium atoms are displaced by 0.078 and 0.088 Å, respectively, out of the plane of their equatorial oxygen and nitrogen atoms toward the axial oxygen atoms of water molecules, which participate in hydrogen-bonding interactions throughout the crystal lattice (Table II).

The lengths of the Rh–O bonds of the axial waters Rh(1)–O(2) (2.311 (3) Å) and Rh(2)–O(1) (2.319 (3) Å) fall in the range quoted for the Rh–O_{ax} bonds. The values of the angles Rh(1)–Rh(2)–O(1) and Rh(2)–Rh(1)–O(2) (167.9 (1) and 169.3 (1)°, respectively) are significantly different from those found in the complex $Rh_2(O_2CCF_3)_4(H_2O)_2 \cdot 2DTBN$ (178.75 (7)°). The only reason for the nonlinearity of the Rh–Rh–O_{ax} angles can be attributed to the steric interactions between the water molecules and the tolyl fragments. The Rh–N distances range from 1.987 (3) to 1.996 (4) Å and are in agreement with the values found in the complex $Rh_2(Form)_3(NO_3)_2$[5] (mean value 1.965 (17) Å), where the Rh–N bonds are in trans positions with respect to oxygen atoms of the nitrato groups.

Distances and angles within the trifluoroacetate groups (d(C–O) = 1.241 Å, O–C–O = 129.25°) are as expected. The structural features of the formamidinate fragments (d(C–N) = 1.308 (4) Å, N–C–N = 124.6 (4)°) are very similar to those found in the complex $Rh_2(Form)_3(NO_3)_2$ (d(C–N) = 1.33 (2) Å, N–C–N = 123 (1)°); in both compounds the C–N bond distances are short enough to indicate a significant double-bond character of the N–C–N groups.

The other striking structural feature of the title complex is the cisoid arrangement of the formamidinate ligands. While surprising, this arrangement is not unprecedented. It is worthwhile mentioning that, among the mixed-ligand Rh_2^{4+} carboxylato complexes possessing the "lantern" structure, namely $Rh_2(O_2CCH_3)_2(O_2CC(C_6H_5)_3)(CH_3CN)_2$,[2a] $Rh_2(mhp)_2(O_2CCH_3)_2(C_3H_4N_2)_2$ (mhp = 6-methyl-2-hydroxypyridine),[2b] and $Rh_2(O_2CCH_3)_2[(C_6H_5)_2P(C_6H_4)]_2 \cdot 2L$ (L = CH_3OH, pyridine[2c]), only the hydroxypyridine derivative exhibits the trans configuration. For the first compound Cotton suggested that the cisoid arrangement of the triphenylacetate groups could be due to attractive contacts between the two phenyl fragments of adjacent C–CPh_3 groups. Concerning the title complex, we cannot invoke interligand tolyl–tolyl contacts because these in all cases are greater than their van der Waals sums. The reason for the cisoid arrangement remains inexplicable, but steric rather than electronic factors might account for the cis disposition of the formamidinate ligands. The use of space-filling molecular models indicates that the transoid form of the hypothetical complex $Rh_2(Form)_2(O_2CCF_3)_2$ with vacant axial sites is less sterically congested than the cisoid one. The stabilization of the cisoid form of **1**, hence, could be due only to the axial coordination of the water molecules or to the consequent formation of intermolecular hydrogen bonds, which are hindered in the transoid form.

Electrochemistry. Figure 2 shows the cyclic voltammetric responses at a platinum electrode given by complex **1** in dichloromethane (Figure 2a) and in acetonitrile (Figure 2b) solutions, respectively. As can be seen, complex **1** gives rise in MeCN solvent to three subsequent anodic processes, at peaks A, C, and E, respectively, the most anodic of which is masked by the solvent cutoff in CH_2Cl_2. In both solvents controlled-potential coulometric experiments performed at the potential of the first anodic process (about 200 mV more anodic than the peak potential of peak A) indicate that it consumes 1 mol of electrons/mol of starting compound. The electrogenerated monocation $[1]^+$ gives rise in cyclic voltammetry just to the cathoanodic peak system B/A.

Cyclic voltammetric tests at scan rates v varying from 0.02 to 50 V s^{-1} show the following features in MeCN: the peak-current ratio $i_p(A)/i_p(B)$ is constantly equal to unity; the $i_p(A)/v^{1/2}$ current function is constant; the difference ΔE_p ($\Delta E_p = E_p(A) - E_p(B)$) is constantly equal to 60 mV. All these parameters are diagnostic for a one-electron reversible charge transfer, uncomplicated by following chemical reactions. The same characteristics hold in

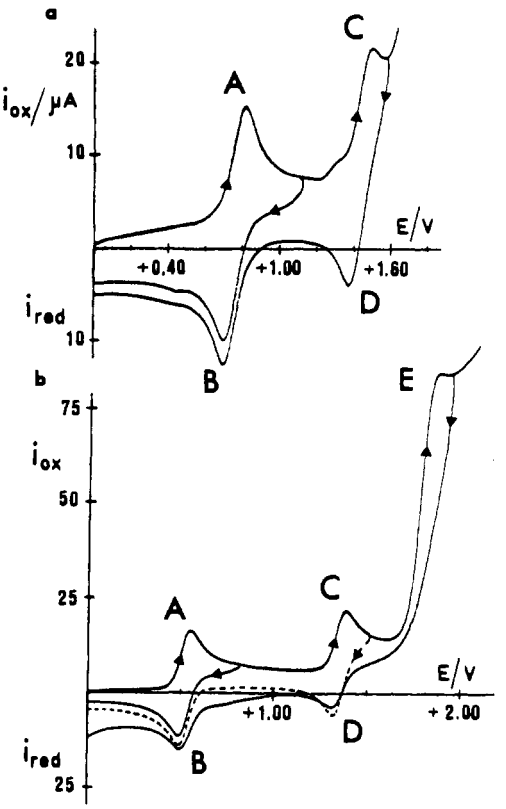

Figure 2. Cyclic voltammograms recorded at a platinum electrode under the following experimental conditions: (a) dichloromethane solution containing **1** (8.6×10^{-4} mol dm^{-3}) and $[NBu_4]ClO_4$ (0.1 mol dm^{-3}); (b) acetonitrile solution containing **1** (8.2×10^{-4} mol dm^{-3}) and $[NEt_4]ClO_4$ (0.1 mol dm^{-3}). Scan rate 0.2 V s^{-1}.

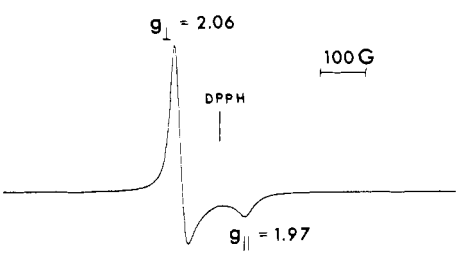

Figure 3. ESR spectrum at room temperature (≃20 °C) of electrogenerated (at +1.06 V) $[1]^+$ in CH_2Cl_2–$[NBu_4]ClO_4$ (0.1 mol dm^{-3}), after solvent evaporation.

CH_2Cl_2 solvent, except for the ΔE_p term, which tends to depart from the theoretical value of 59 mV with scan rate, likely because of a slower heterogeneous electron transfer.

The deep blue product obtained from the exhaustive electrolysis at the first anodic process was examined by ESR spectroscopy. In CH_2Cl_2 solution, with $[NBu_4]ClO_4$ supporting electrolyte, at room temperature (23 °C) it gives an isotropic signal with g = 2.04 (ΔH_{iso} = 29.3 G). The signal obtained at room temperature in the solid powder, after solvent evaporation, is reported in Figure 3.

The anisotropic feature of the spectrum is indicative of an axially symmetric pattern, with the $g_\parallel$ signal due to an unresolved hyperfine structure. This absorption line could be interpreted in terms of an 1:2:1 triplet due to the interaction between the unpaired electron and the rhodium nuclei ($I = {}^1/_2$). A similar behavior has been illustrated in the frozen-glass spectra of monocationic dirhodium acetamidates[13] and mixed carboxylate–acetamidates.[4]

As regards the second anodic process, it is evident from the cyclic voltammogram that it also involves a one-electron reversible

(13) Bear, J. L.; Zhu, T. P.; Malinski, T.; Dennis, A. M.; Kadish, K. M. *Inorg. Chem.* **1984**, *23*, 674.

Table IV. Comparison among the Formal Electrode Potentials (V, vs. SCE) for the Anodic Oxidation of $Rh_2(Form)_2(O_2CCF_3)_2(H_2O)_2$ and Those of Related Dirhodium(II) Complexes

	$E°$ (in MeCN)			$E°$ (in CH_2Cl_2)			
complex	$Rh^{II}Rh^{II}/Rh^{III}Rh^{II}$	$Rh^{III}Rh^{II}/Rh^{III}Rh^{III}$	K_{com}	$Rh^{II}Rh^{II}/Rh^{II}Rh^{III}$	$Rh^{II}Rh^{III}/Rh^{III}Rh^{III}$	K_{com}	ref
$Rh_2(O_2CCF_3)_4$	out of the anodic limit			$\simeq$+1.8			3a, 13
$Rh_2(ONHCCF_3)_4$	+1.09			$\simeq$+1.1			3a, 13
$Rh_2(phosphino)_2(O_2CCH_3)_2$[a]				+1.0			2c
$Rh_2(acam)_2(O_2CCH_3)_2$[b]	+0.62						4, 16
$Rh_2(Form)_2(O_2CCF_3)_2(H_2O)_2$[c]	+0.52	+1.36	2×10^{14}	+0.76	+1.44	3×10^{11}	present work
$Rh_2(acam)_4$[b]	+0.15	+1.41	2×10^{21}				16
$Rh_2(PhNpy)_4$				−0.05	+0.6	1×10^{11}	15
$Rh_2(3,5\text{-}Mepz)_4$				+1.1[d]			3c

[a] phosphino = $(C_6H_5)_2P(C_6H_4)$. [b] acam = $ONHCCH_3$. [c] Form = $(p\text{-}CH_3C_6H_5N)_2CH$. [d] Peak potential for an irreversible process.

charge transfer, generating an apparently stable dicationic species. This picture is quite reminiscent of the voltammetric behavior of a few amidate, mixed carboxylate–amidate, and tetrakis(anilinopyridine) dirhodium complexes,[3b,4,13-16] in which the two steps have been attributed to the subsequent generation of $Rh^{II}Rh^{III}$ and $Rh^{III}Rh^{III}$ complexes, respectively. However, controlled-potential coulometric tests, performed in MeCN–0.1 M $NaClO_4$ solution at the potentials of peak C, indicate it involves a multielectron process (even after the slow consumption of 5 mol of electrons/mol of **1** the residual current is significantly higher than the background current). The resulting solution is acidic. The IR spectrum of the greenish solid obtained after crystallization from CH_2Cl_2 clearly shows that the oxidized product does not contain the trifluoroacetate groups while the formamidinate infrared bands, although still present, seem different from those of the starting complex and are likely to be attributed to the oxidation of the coordinated ligands. In fact it must be taken into account that free *N,N'*-di-*p*-tolylformamidine is electroactive, and it undergoes for instance in MeCN solution an irreversible one-electron charge transfer at E_p = +0.95 V.

All these findings indicate that the $Rh^{III}Rh^{III}$ complex is stable only for the short times of cyclic voltammetry and then it undergoes redox changes, which modify its composition and lead to further oxidizable products, which we were unable to identify. It must be noted also that tetraacetamides[16] and tetrakis(phenylacetamidates)[13] give rise to unstable $Rh^{III}Rh^{III}$ species.

Table IV reports the formal electrode potential for the couples $[\mathbf{1}]^+/\mathbf{1}$ and $[\mathbf{1}]^{2+}/[\mathbf{1}]^+$ in the two cited solvents, together with those of some interrelated dirhodium(II) complexes. Also reported are the relevant computed comproportionation constants, K_{com}, which reflect the extent of the stability of the mixed-valent $Rh^{II}Rh^{III}$ species. According to Gagnê's suggestions.[17] if one considers the equilibrium

$$Rh^{II}Rh^{II} + Rh^{III}Rh^{III} \underset{}{\overset{K_{com}}{\rightleftharpoons}} 2Rh^{II}Rh^{III}$$

the following relation holds:

$$K_{com} = e^{nF\Delta E°/RT}$$

where $\Delta E°$ is the difference between the formal potentials of the two one-electron-oxidation steps.

Previous studies[13] have shown that the substitution of NH for O (from tetracarboxylates to tetraamidates) in dirhodium complexes lowers the oxidation potential by about 700 mV. As can be seen also, the substitution of carboxylate groups for electron-donating phosphino groups makes the oxidation process more favorable. The more effective lowering of the oxidation potential operative in the compound presented here has to be explained in the following terms: (a) With respect to tetrakis(trifluoroacetamidates) it contains the same number of nitrogen atoms (four) substituting the oxygen atoms of tetrakis(trifluoroacetates), but each nitrogen atom bears an electron-donating *p*-tolyl group; in addition the whole ligand lacks of two electron-withdrawing CF_3 groups. Electron-donating groups favor and electron-withdrawing groups disfavor the thermodynamic access to the monocation dimer. (b) With respect to the mixed acetamidato–acetato complex, it contains two more nitrogen atoms bearing electron-donating groups, but it also contain two more electron-withdrawing CF_3 groups. On the other hand, just the presence of these CF_3 groups makes the formamidinato complex less easily oxidizable than the tetraacetamidato derivative, the number of nitrogen atoms being equal. Finally, the substitution of eight O for eight N atoms in tetrakis(anilinopyridine) product causes the strongest lowering of the oxidation potential, even if this cannot be assumed as a general criterion, since the eight-nitrogen-coordinated tetrapyrazolato complex[3c] is notably more difficult to be oxidized.

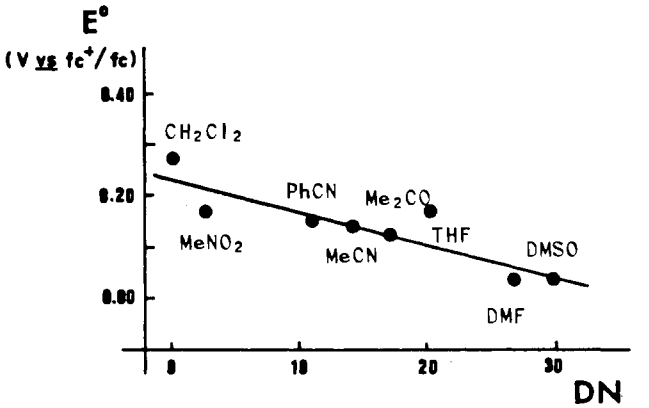

Figure 4. Dependence of the formal electrode potential of the $[\mathbf{1}]^+/\mathbf{1}$ couple on the donor number of the solvent.

We have tested the ability of **1** to undergo the above-described one-electron-oxidation process in several solvents. In all solvents this process appears as a reversible charge transfer, except for $MeNO_2$ and THF, where, as in CH_2Cl_2, it appears as a quasi-reversible step. Figure 4 shows a plot of the relevant oxidation potentials as a function of the well-known Gutmann donor number.[18] In order to eliminate variable diffusion potentials arising at the aqueous–nonaqueous reference electrode, ferrocene was used as an internal standard, so that potential values required to account for solvent effects are referred to the ferrocenium–ferrocene redox couple.

As in the case of tetracarboxylates[19] and tetraamidates[13] nonbonding solvents stabilize the $Rh^{II}Rh^{II}$ species, whereas bonding solvents favor the access to the mixed-valence $Rh^{III}Rh^{II}$ species. In a comparison of the slopes of the straight lines relevant to tetracarboxylates and tetraamidates with that reported in Figure 4 it can be stated that the HOMO level of our compound is destabilized by the axial binding ability of the solvent much less

(14) Duncan, J.; Malinski, T.; Zhu, T. P.; Hu, Z. S.; Kadish, K. M.; Bear, J. L. *J. Am. Chem. Soc.* **1982**, *104*, 5507.
(15) Tocher, D. A.; Tocher, J. H. *Inorg. Chim. Acta* **1985**, *104*, L15.
(16) Zhu, T. P.; Ahsan, M. Q. Malinski, T.; Kadish, K. M.; Bear, J. L. *Inorg. Chem.* **1984**, *23*, 2.
(17) Gagnê, R. R.; Spiro, C. L.; Smith, T. J.; Hamann, C. A.; Thies, W. R.; Shiemke, A. K. *J. Am. Chem. Soc.* **1981**, *103*, 4073.
(18) Mayer, U. *Coord. Chem. Rev.* **1976**, *21*, 159.
(19) Das, K.; Kadish, K. M.; Bear, J. L. *Inorg. Chem.* **1978**, *17*, 930.

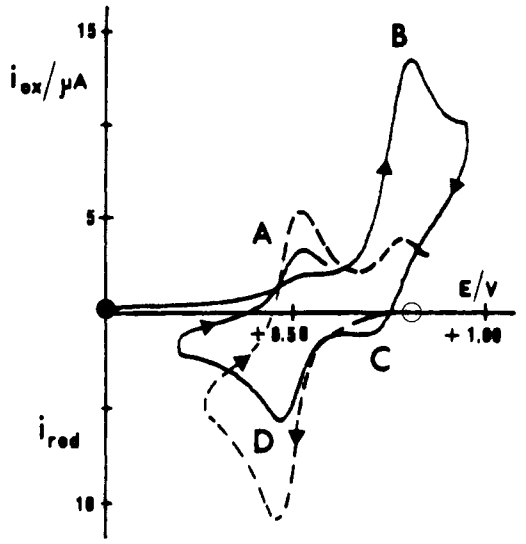

Figure 5. Cyclic voltammograms at a platinum electrode recorded in Me_2SO: (—) solution containing **1** (9.2×10^{-4} mol dm^{-3}) and $[NEt_4]ClO_4$ (0.1 mol dm^{-3}); (---) solution after exhaustive one-electron oxidation at +0.90 V$^-$ ((●) starting potential for the anodic scan; (○) starting potential for the cathodic scan).

(about 50%) than those of tetracarboxylates and tetraamidates.

It must be noted that linear regression analysis of data in Figure 4 gives a correlation coefficient of −0.88, denoting an incomplete ability of the donor number to account for solvent effects. In order to better rationalize solvent effects on redox potentials, we have recently proposed[20] a multiparameter analysis, which takes into account hydrogen-bonding-donor (or Lewis acidity) parameters, and polarity–polarizability parameters. We shall present elsewhere this type of statistical treatment;[21] however, here we wish to show that even by simply considering one basicity parameter (the donor number, DN) and one acidity parameter (the Dimroth–Reichardt parameter, $E_T(30)$)[22] a better correlation can be achieved. In fact the following equation holds:

$$E_{1/2}\,(V) = 0.6618 - 0.0063\ DN - 0.0099\ E_T(30)$$

A squared correlation coefficient of 0.970 has been found (which is highly significative for a multiregression with two independent variables), and each coefficient is significative at an extent higher than 99%, as computed by the Student t test.

The formal electrode potential for the $Rh^{III}Rh^{II}/Rh^{II}Rh^{II}$ couple assigned in Me_2SO deserves some discussion. Figure 5 (solid line) shows the cyclic voltammetric behavior of **1** in Me_2SO solution. Two anodic peaks, A and B, are displayed in the forward scan, with B more prominent than A. It is however evident that in the reverse scan peak D, which is directly associated to peak A, tends to increase in magnitude in respect to peak C, which is directly associated to peak B. This picture suggests that the species oxidized at peak B undergoes a chemical reaction leading to a species that is reduced at peak D and oxidized at peak A, i.e. to the oxidized form of the species initially present in a minor amount.

Macroelectrolysis experiments performed in correspondence to the more anodic process (at +0.90 V) confirm this result; in fact after the one-electron oxidation, the resulting deep violet solution displays in cyclic voltammetry the cathoanodic peak system D/A, as shown in Figure 5 (dashed line). In addition, room-temperature ESR tests on this electrolyzed solution give the previously discussed isotropic signal ($g = 2.04$) attributed to the $Rh^{III}Rh^{II}$ species. At least two hypotheses can account for the presence of two different $Rh^{II}Rh^{II}$ species in Me_2SO solution, and both are centered on the solvent axial coordination. The first one is based on the presence of both Me_2SO monoadduct and Me_2SO bisadduct, in different amounts, with the monoadduct less easily oxidizable than the bisadduct.[23,24] The second one invokes two dimeric species with the solvent ligated with two different coordinations; in the neutral dimer the rhodium atoms are preferentially bonded to Me_2SO through sulfur atoms, while in the monocationic dimer the rhodium atoms are preferentially bonded through oxygen atoms.[4] We have chosen the potential of the couple A/D (+0.49 V) as representative of the standard potential of the $[\mathbf{1}]^+/\mathbf{1}$ couple, rather than the potential of the couple B/C (+0.75 V), taking into account that for amidates[13] and mixed carboxylate–amidates[4] the standard potential in Me_2SO is usually higher than expected, because the electrogenerated cationic species displaying the cathoanodic peak system A/D is the most stable and is responsible for the paramagnetism of the $Rh^{III}Rh^{II}$ dimer.

Concluding Remarks

The substitution of a pair of trifluoroacetate groups by formamidinate groups in the complex $Rh_2(O_2CCF_3)_4$ leads to structural and electronic alterations. From the structural point of view an elongation of the Rh–Rh bond distance is observed. This is attributable to the constraining effect of the formamidinate ligands, while the steric interactions, which are responsible for the distortions previously described, do not hinder the formation of 1:2 adducts, as occurs for instance in the mixed-ligand complex $Rh_2(O_2CCH_3)_2(mhp)_2(C_3H_4N_2)$.

Finally, the synthesis of the complex $Rh_2(Form)_2(O_2CCF_3)_2(H_2O)_2$ is of interest for two reasons: (i) the procedure of synthesis reported here can be extended to other binuclear rhodium(I) complexes containing the appropriate ligands; (ii) preliminary results show that the trifluoroacetate groups can be easily displaced by anionic ligands. Thus, the title complex can be the precursor of a range of mixed-ligand Rh_2^{4+} complexes, which so far have not been prepared by a synthetic procedure of general applicability.

Acknowledgment. We thank the CNR and the Public Education Ministry for financial support. We are also indebted to Prof. R. Basosi for ESR spectra.

Registry No. **1**, 105164-41-8; $\mathbf{1}^+$, 105164-45-2; $\mathbf{1}^{2+}$, 105164-46-3; **2**, 105164-42-9; **3**, 105182-87-4; **4**, 105164-43-0; **5**, 105164-44-1; $[Rh(C_8H_{12})(Form)]_2$, 81229-43-8; Rh, 7440-16-6.

Supplementary Material Available: Listings of distances and angles associated with the tolyl and trifluoroacetate fragments (Table V), hydrogen atom parameters (Table VI), and temperature factors (Table VII) (3 pages); a listing of structure factors (31 pages). Ordering information is given on any current masthead page.

(20) Seeber, R.; Zanello, P. *J. Chem. Soc., Dalton Trans.* **1985**, 601.
(21) Seeber, R.; Zanello, P.; Piraino, P. work in progress.
(22) Reichardt, C. *Angew. Chem., Int. Ed. Engl.* **1979**, *18*, 98.
(23) Drago, R. S.; Tanner, S. P.; Richman, R. M.; Long, J. R. *J. Am. Chem. Soc.* **1979**, *101*, 2897.
(24) Bottomley, L. A.; Hallberg, T. A. *Inorg. Chem.* **1984**, *23*, 1584.